Available online at www.sciencedirect.com
SCIENCE DIRECT®
PERGAMON
International Journal of Heat and Mass Transfer 46 (2003) 2459–2469
International Journal of HEAT and MASS TRANSFER
www.elsevier.com/locate/ijhmt

Two-dimensional simulation of turbulent flow and transfer through stacked spheres

Simulation bi dimensionnelle des écoulements et des transferts dans un empilement de sphères

Graciela Alvarez [a,*], Pierre-Emmanuel Bournet [b,1], Denis Flick [b,2]

[a] *INRA, ENSIA, INA-PG CEMAGREF, UMR GENIAL Génie Industriel Alimentaire (Cemagref Unité de Recherche Génie des Procédés Frigorifiques), Parc de Tourvoie B.P. 44, 92185 Antony Cedex, France*
[b] *UMR GENIAL Génie Industriel Alimentaire (Institut National Agronomique Paris-Grignon), 16, rue Claude Bernard, 75005 Paris, France*

Received 23 May 2001; received in revised form 13 October 2002

Abstract

We propose a one-equation model for two-dimensional turbulent flow through porous media. The momentum equation is derived from the space averaging of Navier–Stokes equations, leading to the so-called Darcy–Forchheimer equations. In the turbulent kinetic energy transport equation, the production term is assumed to be proportional to the cube of velocity. The dissipation term is not estimated with a transport equation, it is explicitly given by a law involving turbulent kinetic energy and velocity. The model requires only four experimentally determined parameters. The local Nusselt number was correlated to local Reynolds number, and to local turbulence intensity. Good agreement between the simulated and the experimental local Nusselt number is obtained.

Résumé

Un modèle d'écoulement turbulent à une équation a été proposé pour simuler l'écoulement bi-directionnel en milieu poreux constitué de sphères. L'équation de quantité de mouvement -ou équation de Darcy–Forchheimer- est obtenue à partir de la moyenne spatiale des équations de Navier–Stokes. Dans l'équation de transport de l'énergie cinétique turbulente, le terme de production est supposé proportionnel au cube de la vitesse. Le terme de dissipation de cette équation n'est pas estimé par une équation de transport mais est donné en fonction de la vitesse et de l'énergie cinétique turbulente. Le modèle ne comporte que quatre paramètres qui sont déterminés par voie expérimentale. On établit ensuite une corrélation entre le nombre de Nusselt local, le nombre de Reynolds et le taux de turbulence. Un bon accord est obtenu entre les résultats expérimentaux et les résultats numériques.

Keywords: Airflow porous media; Turbulence model; One-equation model; Aerodynamic measurements; Parameters identification; Heat transfer coefficient
Mots-clés: Écoulement d'air; Milieu poreux; Turbulence; Modèle à une équation; Mesures aérodynamiques; Identification de paramètres; Coefficient de transfert

* Corresponding author. Tel.: +33-1-40-96-60-17; fax: +33-1-40-96-60-75.
E-mail addresses: graciela.alvarez@cemagref.fr (G. Alvarez), bournet@inapg.inra.fr (P.-E. Bournet), flick@inapg.inra.fr (D. Flick).
[1] Tel.: +33-1-44-08-72-08; fax: +33-1-44-08-16-66.
[2] Tel.: +33-1-44-08-72-39; fax: +33-1-44-08-16-66.

0017-9310/03/$ - see front matter
doi:10.1016/S0017-9310(02)00546-X

Nomenclature

a	constant in Eq. (6)
b	constant in Eq. (6)
c	constant in Eq. (6)
C_1	parameter of the model in Eq. (2) (m^{-2})
C_2	parameter of the model in Eq. (2) (m^{-1})
C_3	parameter of the model in Eq. (5) (m^{-1})
C_4	parameter of the model in Eq. (5) (m^{-1})
h	heat transfer coefficient at the interface air-product ($W\,m^{-2}\,K^{-1}$)
h_r	equivalent heat transfer coefficient for radiation ($W\,m^{-2}\,K^{-1}$)
k	turbulent kinetic energy ($m^2\,s^{-2}$)
Nu	Nusselt number (hD/λ)
p	pressure (Pa)
Pr	Prandtl number
Re	modified Reynolds number $\rho vD/\mu(1-\phi)$
Tu	turbulence intensity $Tu=\sqrt{2k}/v$
u	local instantaneous air velocity in the porous medium ($m\,s^{-1}$)
$\overline{u}$	time averaged local air velocity in the porous medium ($m\,s^{-1}$)
u'	fluctuation of instantaneous local air velocity ($u-\overline{u}$) ($m\,s^{-1}$)
$\langle u\rangle$	space averaged instantaneous air velocity ($m\,s^{-1}$)
v	superficial air velocity $v=\langle\overline{u}\rangle=\overline{\langle u\rangle}$ ($m\,s^{-1}$)

Greek symbols

α	under-relaxation factor
α_p	thermal diffusivity of the product ($m^2\,s^{-1}$)
ε	dissipation rate of the turbulent kinetic energy $m^2\,s^{-3}$
λ	thermal conductivity of the air ($W\,m^{-1}\,K^{-1}$)
μ	dynamic viscosity of the air ($kg\,m^{-1}\,s^{-1}$)
ϕ	void fraction

Subscripts

est	referred to estimated quantities
meas	referred to measured quantities
t	iteration index in the numerical procedure
x	referred to x-direction
0	referred to value upstream of the porous medium
∞	referred to equilibrium value

1. Introduction

Forced convection cooling or heating of agricultural products stacked inside a small container induces major heterogeneities in their treatment. This is the case, for instance, with fruits or vegetables stored in cold chambers. Products located behind blind walls may not be sufficiently cooled. This can lead to microbial proliferation and consequent rotting. Moreover, products exposed to high air velocities may be subject to an unwanted desiccation [1]. Poor temperature management of a harvest can lead to its deterioration or even to its complete loss.

The heterogeneity of treatment results from the heating of the air as it passes trough the products and from the variations in the heat transfer coefficient between the air and the surface of the products. The heat transfer coefficient for a given product stack of identical items (same shape and same average size) is a function of airstream characteristics such as velocity and turbulence.

A few studies have been conducted on airflows through stacked items. Beurkema and Bruin [2] and Talbot et al. [3], using potatoes and oranges respectively, established a numerical model to predict airflow and heat transfer inside large containers of fruit and vegetables. Their approach assumes that the medium behaves like a porous medium and they use the Ergun equation which relates the pressure drop to the superficial velocity and involves coefficients based on the void fraction ϕ. In both studies, the predictions were verified using product temperature measurements.

The above studies can predict the mean airflow but do not take turbulence into account. However, free stream turbulence is known to have a major influence on transfer phenomena [4,5]. Comings et al. [5] have shown, for instance, that the Nusselt number Nu increases by 25% when turbulence rises from 1% to 7%. Most studies however, deal with turbulence around a single object and only a few concern turbulence in stacked objects, for instance in a tubular heat exchanger [6,7]. For bins filled with spheres, Alvarez and Flick [8] have recorded velocity maps that exhibited considerable heterogeneity. They also shown that a strong turbulence intensity, up to 50%, is generated by vortices in the wake of the spheres. Some models have recently been developed to take account of turbulence in porous media [9–11]. All these models rely on a two-equation macroscopic turbulence approach with a k–ε closure (see also Section 2). However, they require the determination of a set of unknown constants and often involve costly computing.

This study establishes a model based on the mass, momentum and turbulent kinetic energy transport equations to describe turbulent flows in porous media. A correlation is then established to estimate the heat transfer coefficient as a function of mean velocity and turbulence intensity Tu. A complete description of the

model is first given. This is followed by a description of the experimental procedure used to determine the four unknown constants required by the model. Finally, a particular geometry: a "baffle arrangement", is investigated.

2. Numerical modelling

It is known that high-velocity flows in porous media lead to turbulence within the pores and that highly chaotic structures develop when the pore-Reynolds number (based on the pore size and velocity) becomes $Re > 300$. Velocity measurements with a hot wire anemometer confirm the existence of turbulence in packed beds [8]. There are two main differences between flow through porous media and turbulent free-stream flow: the size of the eddies is limited by the pore size- and additional drag (viscous and form) forces effects are induced by the porous solid matrix.

This section presents the main steps taken to derive a macroscopic k-model for incompressible turbulent flow in porous media. The attention is drawn to the theoretical background and to the specificities of our approach.

2.1. Modelling background

The first step was to predict the pressure and velocity within the porous medium. The approach most commonly used for laminar flows was first described by Darcy, who postulated that the pressure drop within the medium is due to viscous stress and is proportional to the velocity. However Darcy's law is not valid for high-velocity flows and a correction term must be included to take account of inertial effects. This term, is known as the Forchheimer term and is a quadratic function of the velocity. Ergun [12] established empirical expressions for the constants appearing in the momentum equation, involving the porosity of the medium, the viscosity and the density of the fluid and mean equivalent diameter of the product. He validated his expressions for the case of stacked spheres.

Two approaches for defining turbulent kinetic energy and for establishing turbulent kinetic energy transport equation were found in the literature. The first was developed by Antohe and Lage [10], who spatially average the Navier–Stokes equations and then derive the time average of the obtained set of equations. They define the turbulent kinetic energy as $k' = \frac{1}{2}\overline{\langle \vec{u} \rangle'^2}$. The transport equation that they obtain indicates that for a one-dimensional flow, k' reduces to 0 when the flow is established, which means that velocity fluctuations—corresponding to "vortices" larger than the porosity scale—decay and vanish. A second approach was developed by Nakayama and Kuwahara [11] who first time average the Navier–Stokes equations leading to the Reynolds equations. They then take the spatial average of the obtained set of equations and establish an equation for the turbulent kinetic energy k and the dissipation rate ε. Here k is defined as $k = \frac{1}{2}\frac{\overline{\langle \vec{u}'^2 \rangle}}{\phi}$. Given this definition, they shown that k reaches a constant value k_∞ when a one-dimensional flow is established, which means that on penetrating the porous medium, turbulence inside the pores reaches a balance between production and dissipation. The latter approach is used in our study as it considers a kind of turbulence generated by the porous medium. This type of turbulence is suspected of having a strong influence on transfers between the air and the products.

2.2. Governing equations

Our aim was to establish a simple model, valid for 2D and 3D flows, that would gives a good approximation of the turbulent kinetic energy and would predict the heat transfer coefficient through stacked objects. The following model was derived from the approach developed by Nakayama and Kuwahara [11]. Only one equation is used for closure i.e. the dissipation rate appearing in the turbulent kinetic energy transport equation is directly expressed as a function of the turbulent kinetic energy and of the velocity magnitude. For reasons of simplicity and to reduce the number of parameters to be determined, we use a semi-empirical approach. The suggested model can then be adapted to different shapes of products and various configurations of arrays.

2.2.1. Assumptions

It is assumed in this study that:

- The flow is incompressible.
- The flow is steady.
- The macroscopic inertial term (or macroflow development term) as defined by Kaviany [13]: $\frac{\rho}{\phi} v \cdot \nabla v$, is negligible in the momentum equations. Indeed in our case, the macroscopic kinetic energy: $\frac{1}{2}\rho v^2$, is very small compared to the pressure drop throughout the porous media (the ratio is less than 1%).
- The microscopic inertial forces (microflow development) are taken into account (Ergun term).
- The macroscopic or bulk viscous shear stress diffusion term (or Brinkman term): $\frac{\mu}{\phi}\nabla^2 v$, is negligible. Indeed in our case, the Reynolds number (defined with pore velocity and dimension) which compares viscous forces and (microflow) inertial forces is high ($Re > 10^4$).

Given these assumptions, the number of unknown parameters is reduced to four.

2.2.2. Macroscopic continuity, momentum and turbulent kinetic energy equations

The following macroscopic equations are obtained for turbulent flows. The velocity v that appears is both temporally and spatially averaged: $\vec{v} = \overline{\langle \vec{u} \rangle}$. Assuming that the flow is steady, we also have $\overline{\langle \vec{u} \rangle} = \langle \vec{u} \rangle$.

1. The mass conservation equation is

$$\vec{\nabla} \cdot \vec{v} = 0 \tag{1}$$

2. The momentum conservation equation is derived from Forchheimer-extended Darcy's law:

$$-\vec{\nabla} p = C_1 \mu \vec{v} + C_2 \rho |\vec{v}| \vec{v} \tag{2}$$

The first term on the right-hand side (Darcy's term) accounts for the microscopic viscous drag while the second term accounts for the form drag which is due to inertial effects (direction changes) inside the pores and to turbulent dissipation. For the particular case of stacked spheres, Ergun [12] suggested the following expressions for the constants C_1 and C_2:

$$C_1 = 150 \frac{(1-\phi)^2}{\phi^3 D^2}$$

$$C_2 = 1.75 \frac{(1-\phi)}{\phi^3 D}$$

where D is the equivalent diameter of the product and ϕ the void fraction. For the purpose of our study which considers stacked spheres in alignment (whereas Ergun studied randomly stacked spheres), C_1 and C_2 are estimated experimentally.

3. Turbulent kinetic energy k: In view of the work of Nakayama and Kuwahara [11], we define the turbulent kinetic energy as: $k = \frac{1}{2} \frac{\overline{\langle \vec{u}'^2 \rangle}}{\phi}$. As they do, we neglect the diffusion term and assume that the production term: P_k, is proportional to the cube of velocity. The latter term can be interpreted as the transformation of part of the kinetic energy of the mean flow into fluctuation energy due to drag forces. For steady state flow:

$$\vec{\nabla} \cdot k\vec{v} = P_k - \epsilon \tag{3}$$

with $P_k = C_3 |\vec{v}|^3$.

Nakayama and Kuwahara [11] proposed $C_3 = (39(1-\phi)^{5/2}/D)|\vec{v}|^3$.

They also proposed a transport equation for the dissipation rate of following kind:

$$\vec{\nabla} \cdot \epsilon \vec{v} = C_5 |\vec{v}|^4 - C_6 \frac{\epsilon^2}{k} \tag{4}$$

For one-directional fully developed flow (far enough from inlet), Eqs. (3) and (4) lead to equilibrium between production and dissipation: $\epsilon_\infty = P_{k\infty} = C_3 v^3$. Kinetic turbulent energy reaches an equilibrium value proportional to square of velocity: $k_\infty = \frac{C_6 C_3^2}{C_6} v^3$. This means that the turbulence intensity, defined as $Tu = \frac{\sqrt{2k}}{v}$, becomes independent of the velocity far from the inlet.

However the use of Eq. (4) would introduce two more coefficients C_5 and C_6 which are difficult to identify. This is the reason why we propose a simplified approach assuming that the dissipation of turbulent kinetic energy follows a fist order law: $\epsilon = \frac{k}{k_\infty} \epsilon_\infty = \frac{C_5}{C_3 C_6} kv = C_4 kv$.

Eq. (3) becomes then:

$$\vec{\nabla} \cdot k\vec{v} = C_3 |\vec{v}|^3 - C_4 k |\vec{v}| \tag{5}$$

The last term of this equation is similar to the one suggested by Green [9,14] in order to take into account supplementary dissipation generated by obstacles in turbulent flow and it is consistent with that derived by Wilson [15] in case of isotropic turbulence. For flow through vegetation, Green considered additionally that $C_2 = C_3$ and $C_4 = 4C_2$.

In conclusion we use only one equation involving two parameters to predict turbulence intensity. In our case the characteristic length scale of turbulence in the porous medium is closely linked to the size of the pores and particles. This justifies partially that we do not use a second equation (transport of ϵ) which can be viewed as the transport of the length scale of the eddies.

4. Heat transfer correlation: The heat transfer coefficient is assumed to depend on the velocity and the turbulence intensity, according to the law:

$$Nu = aRe^b Pr^{1/3}(1 + cTu) \tag{6}$$

Here $Nu = \frac{hD}{\lambda}$ is the Nusselt number, where λ is the air conductivity and h is the heat transfer coefficient (mean value for the surface of one sphere). $Re = \rho v D/\mu(1-\phi)$ is the modified Reynolds number which takes account of the mean interstitial velocity and the mean hydraulic pore diameter. Exponent b of the Reynolds number remains to be determined. Pr is the Prandtl number. Its exponent 1/3 was obtained for isolated objects and its value for an air flow is 0.71.

The influence of local turbulence intensity is taken into account by the term $(1 + cTu)$, where c is a constant. In the case of stacked objects, the heat transfer coefficient (Nusselt number) is often related to velocity (Reynolds number) and row position (n). Here, we propose to take row position into account indirectly by the local turbulence intensity which increases row after row.

In the literature, for single object, heat transfer enhancement due to turbulence is taken into account by several correlation involving the turbulence intensity: $Tu = \frac{\sqrt{2k}}{v}$ [4], or its product with Reynolds number: $Tu \cdot Re$ [16], or $Tu\sqrt{Re}$ ([17,18]).

On the one hand, for our turbulence model and for one-directional flow, turbulence intensity depends on row position but not on velocity (Reynolds number). On

the other hand, we observed experimentally that the ratio of the heat transfer coefficients between the first row and an other row is almost independent of the air velocity.

Thus we have chosen to express heat transfer enhancement simply by a linear function of the turbulence intensity.

2.2.3. Boundary conditions

When the pressure at the inlet and outlet is known, it is directly imposed in the programme. However, often, only the flow rate is known and the pressure drop between the inlet and the outlet must be adjusted so as to give the expected flow rate. The turbulent kinetic energy k at the inlet is imposed. It is generally very weak compared to the velocity fluctuations generated by the obstacles.

At walls, the normal pressure gradient and velocity are equal to zero (no exchange of mass between the porous medium and the surrounding medium).

2.3. Numerical procedure

The unknown variables are the pressure p, the velocity field $\vec{v}$ and the turbulent kinetic energy k.

The governing equations are discretized using the finite volume method. They are then solved by reducing the system to successive linear tridiagonal systems. The program was written in Fortran. All calculations were performed using a Sun UltraSparc 60.

In the first stage, Eqs. (1) and (2) are combined giving:

$$\vec{\nabla}\cdot\left(\frac{\vec{\nabla}p}{C_1\mu + C_2\rho|\vec{v}|}\right) = 0 \tag{7}$$

This equation is then solved according to an iterative procedure: from an estimated velocity field at iteration $t-1$, it is possible to calculate a new pressure field at iteration t:

$$\vec{\nabla}\cdot\left(\frac{\vec{\nabla}p_t}{C_1\mu + C_2\rho|\vec{v}_{t-1}|}\right) = 0 \tag{8}$$

A new velocity field is then deduced from Eq. (2):

$$\overrightarrow{v_t} = \frac{\vec{\nabla}p_t}{C_1\mu + C_2\rho|\vec{v}_{t-1}|} \tag{9}$$

To improve the convergence process, an under-relaxation is applied at each iteration. We thus obtain the velocity $\overrightarrow{v_t}$ at iteration t:

$$\overrightarrow{v_t} = \alpha\frac{\vec{\nabla}p_t}{C_1\mu + C_2\rho|\vec{v}_{t-1}|} + (1-\alpha)\vec{v}_{t-1} \tag{10}$$

where α is the under-relaxation factor $\alpha \in [0,1]$. For practical reasons, we took $\alpha = 0.2$.

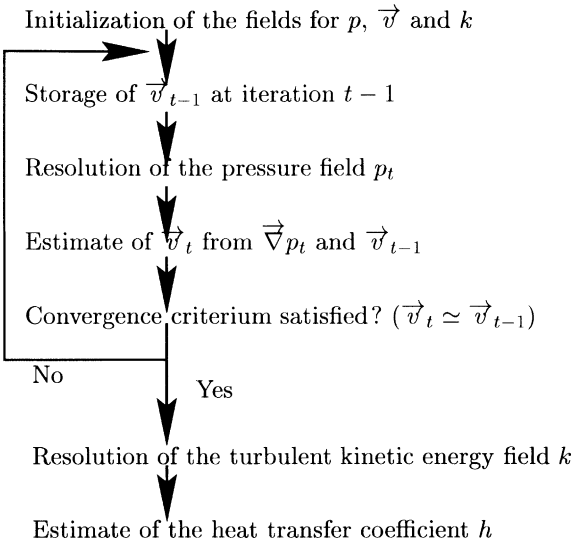

Fig. 1. Algorithm of the one-equation model for flows in porous media.

The mass and momentum equations are discretized according to an implicit centred scheme. The equation for the transport of k (Eq. (5)), however, is discretized according to an upwind scheme as diffusion is neglected. In order to avoid incorrect zigzag pressure field [19], we use a staggered grid: scalar quantities are estimated at the centre of cells and velocity components at the centre of cell faces. The corresponding algorithm is shown in Fig. 1.

3. Description of the experimental device

Experimental determination of the unknown model constants, C_1, C_2, C_3 and C_4, requires detailed measurements of velocity and turbulence in a porous medium.

3.1. Experimental material

The experimental setup is an air-blast tunnel consisting of a rectangular section followed by a converging channel connected to an air extraction duct. The airflow temperature could be kept constant automatically and was maintained at 293 K during our experiments. The air velocity may vary from 0 to $\approx$2.7 m s^{-1}.

The porous medium consists of 75 mm diameter PVC spheres. The corresponding facility is shown in Fig. 2. The device consisted of a plane of spheres with 5 rows in the y-direction (perpendicular to the main flow) and n rows in the x-direction (corresponding to the direction of the main flow). The number of rows in the x-direction, n, could vary between 1 and 5. The spheres were in contact with one another in both the x and y directions. Half

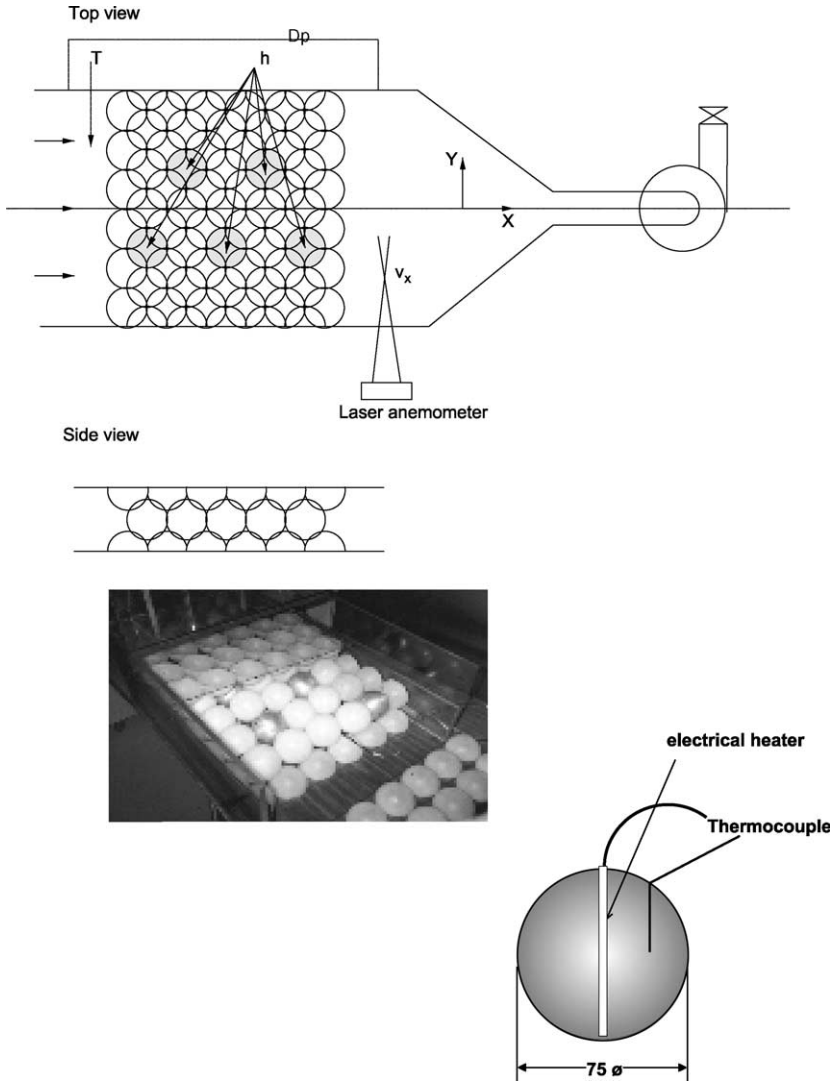

Fig. 2. Device used for experiments.

spheres were stuck to plexiglass sheets above and below this plane and the lateral plexiglass walls, in contact with the complete spheres. Such a configuration, (corresponding to a rectangular stack) is not very far from an infinite medium (for which there would be no plexiglass boundary), as the shear surface between the air and the lateral walls is minimized.

For stacked 75 mm diameter spheres arranged in rectangular parallelepipeds, the theoretical height of the porous medium is 106 mm and the corresponding void fraction is thus $\phi = 0.26$. The observed height is however, 120 mm due to the fact that there was not always perfect contact between adjacent spheres. We therefore considered that the experimental porosity of the device was $\phi = 0.34$.

3.2. Measurements

The pressure drop was measured with to a tilted-tube pressure gauge, for different flow rates, and for different numbers of rows of spheres. The flow rate was measured with an Annubar sensor located in the extraction duct.

Instantaneous velocity was measured upstream and 100 mm downstream of the porous medium in the x-direction, using a laser anemometer. For most of measurements, water droplets of 2×10^{-6} m mean diameter obtained with an ultrasonic spray device were used for seeding. For some experiments incense smoke which contains much smaller particles was also used. Similar results were obtained for mean and RMS of velocity.

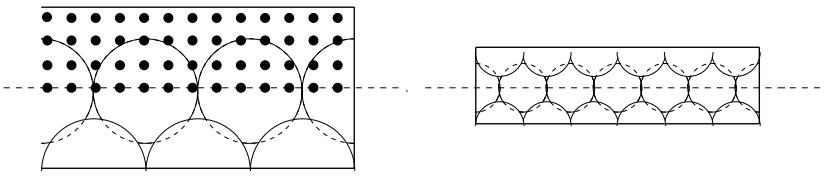

Fig. 3. Location of the velocity measurement points.

As the spheres were arranged symmetrically, we used a measurement grid of 4*13 points located on only a quarter of the section (see Fig. 3).

Local heat transfer coefficient was measured using the stationary method [20,21] for several upstream air velocities: from 0.95 to 2.7 $m\,s^{-1}$. A full description of this method may be found in [22]. It consists of measuring the temperature difference between aluminium spheres heated by Joule effect and the ambient air upstream of each sphere. Indeed each aluminium sphere was equipped with an electrical heater placed at their centre, allowing a constant flux (1415 $W\,m^{-2}$) to be delivered. A Copper–Constantan thermocouple was inserted in the sphere (see Fig. 2).

Both air and sphere temperature measurements were performed using calibrated Copper–Constantan thermocouples. In the case of aluminium spheres, the Biot number $\frac{hD}{\lambda_{alu}}$ is under 0.1 ($h < 200\ W\,m^{-2}\,K^{-1}$, $D = 0.075$ m, $\lambda_{alu} > 200\ W\,m^{-1}\,K^{-1}$), so the temperature of the sphere can be considered as uniform.

The heat flux leaves the sphere primarily by convection. Conduction between spheres could be neglected as the metallic probes were only in contact with plastic spheres and the area in contact with each probe was negligible (see Fig. 2). As far as radiation is concerned, the measured heat transfer coefficient, h, could be compared with an equivalent radiation heat transfer coefficient $h_r = 4e\tau T^3$. The h values ranged from 50 to 150 $W\,m^{-2}\,K^{-1}$, with a maximum h_r value of about 1.4 $W\,m^{-2}\,K^{-1}$ (the maximum sphere temperature was $T = 40$ °C, e: emissivity of polished aluminium ≈0.2, Stefan–Boltzmann constant $\tau = 5.67 \times 10^{-8}\ W\,m^{-2}\,K^{-4}$). In the worst case, i.e. when heat transfer coefficient is around 50 $W\,m^{-2}\,K^{-1}$, the maximum error due to radiation was about 2.8%. Overall, with errors in measuring temperature (±0.1 °C), electrical resistance measurements (±1 Ω) and voltage measurements (±0.015 V), the error calculated for the convection heat transfer coefficient was about 4%.

3.3. Determination of the model constants

3.3.1. Constants C_1 and C_2 of the momentum equation (Darcy–Forchheimer)

To identify constants C_1 and C_2 of Eq. (2), we considered a one-dimensional flow. Our experiments showed that for a flow velocity of the order of 1 $m\,s^{-1}$, the linear term of Eq. (2) is negligible compared to the quadratic term. The pressure drop is therefore proportional to the squared velocity and we set $C_1 = 0\ m^{-2}$. C_2 was then determined through a linear fit from measurements of pressure drops with 1–5 rows and 2 $m\,s^{-1}$ velocity (Fig. 4). The experimental results disclosed a linear behaviour, from which the slope was identified as the C_2 coefficient, with a value of $C_2 = 321\ m^{-1}$. Using Ergun's law, we obtained a slightly higher value: $C_2 = 392\ m^{-1}$. The difference may be due to the fact that if the spheres are precisely arranged, the flow tends to follow preferential paths, thus reducing any loss of kinetic energy due to flow deflections.

3.3.2. Parameters C_3 and C_4 of the turbulent kinetic energy equation

For a one-dimensional flow, velocity is constant and the turbulent kinetic energy follows a decaying exponential law, from the initial value k_0 to the equilibrium value k_∞:

$$\frac{k - k_\infty}{k_0 - k_\infty} = e^{-C_4 x} \tag{11}$$

where k_0 is the turbulent kinetic energy upstream, k_∞ is obtained from Eq. (5), equalizing the right-hand term to 0:

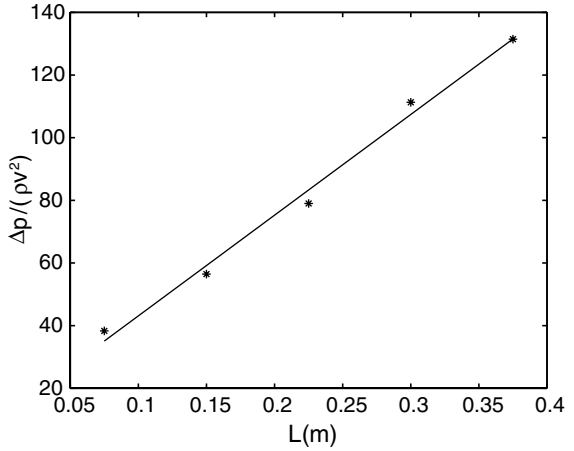

Fig. 4. Pressure drop as a function of the length of the porous medium: experimental results (stars) and linear fit (continuous line).

$$k_\infty = \frac{C_3}{C_4} v^2 \tag{12}$$

For practical reasons, the turbulence could not be measured inside the porous medium but only downstream in flow direction x. From the observations of turbulence decay behind a grid, we assume that the relative decrease of turbulent kinetic energy is a function only of the distance between the outlet of the porous medium and the measurement section. Moreover, as the measurement section was far from the wake or recirculation zones, the turbulence can be considered to be isotropic and therefore proportional to the turbulence measured in the x-direction. Turbulence intensity was defined as $Tu = \sqrt{2k}/v$ and a bulk average over the measurement section was taken in order to obtain a mean value of the measured turbulence intensity in the x-direction:

$$Tu_{x,\mathrm{meas}} = \sqrt{\frac{\int_S \overline{u'^2_{x,\mathrm{meas}}}\,\overline{u_{x,\mathrm{meas}}}\,\mathrm{d}S}{\overline{u_{x,\mathrm{meas}}}^2 \int_S \overline{u_{x,\mathrm{meas}}}\,\mathrm{d}S}} \tag{13}$$

where $u_{x,\mathrm{meas}}$ is the local velocity in the x-direction and $u'_{x,\mathrm{meas}}$ is the velocity fluctuation around the time average value $\overline{u_{x,\mathrm{meas}}}$. We could then write:

$$\frac{Tu^2_{x,\mathrm{meas}} - Tu^2_{x,\mathrm{meas}\infty}}{Tu^2_{x,\mathrm{meas}0} - Tu^2_{x,\mathrm{meas}\infty}} = \frac{Tu^2 - Tu^2_\infty}{Tu^2_0 - Tu^2_\infty} = \frac{k - k_\infty}{k_0 - k_\infty} = \mathrm{e}^{-C_4 x} \tag{14}$$

The upstream turbulence intensity $Tu^2_{x,\mathrm{meas}0}$ was measured and a value of 0.13 was found. The turbulence intensity was also measured downstream for 1, 2 and 3 rows of spheres. Results are reported in Fig. 5. The corresponding nonlinear fit obtained by the Hooke method is also drawn. Values of 0.75 and 21 m^{-1} were found for the asymptote $Tu^2_{x,\mathrm{meas}\infty}$ and for the coefficient C_4 respectively. From the value of C_4, we deduced that the characteristic depth necessary to reach equilibrium between production and dissipation is $1/21 = 0.048$ m.

Coefficient C_3 was then found from the expression suggested by Green [9,14]: $C_3 = C_2$, who assumes that all mechanical energy lost by the mean flow is converted into turbulent kinetic energy before its dissipates as heat. Hence:

$$C_3 = 321\ \mathrm{m}^{-1}$$

3.3.3. Heat transfer

Exponent b of Reynolds number Re (Eq. (6)) is estimated from the average value of the heat transfer coefficient over the rows and for different flow rates:

$$\overline{Nu}^{\mathrm{row}} = aRe^b Pr^{1/3}(1 + c\overline{Tu}^{\mathrm{row}}) = a' Re^b \tag{15}$$

where the superscript $\overline{}^{\mathrm{row}}$ stems for the average over the rows. A linear fit on the logarithm of expression (15) then gives $b = 0.67$.

In the second stage (once b is known), we make a linear fit of $Nu/(Re^b Pr^{1/3})$ as a function of the turbulence measured upstream of the row. Eq. (14) can be written as

$$Tu = \sqrt{Tu^2_\infty - (Tu^2_\infty - Tu^2_0)\mathrm{e}^{-C_4(p-1)\Delta x}} \tag{16}$$

where p is the row index and Δx is the distance between adjacent rows. From Eq. (12) we get

$$Tu_\infty = \frac{\sqrt{2k}}{v} = \sqrt{\frac{2C_3}{C_4}} = 5.53 \tag{17}$$

Coefficients a and c are then determined. The linear fit obtained from the experimental data gives: $a = 0.421$ and $c = 0.059$.

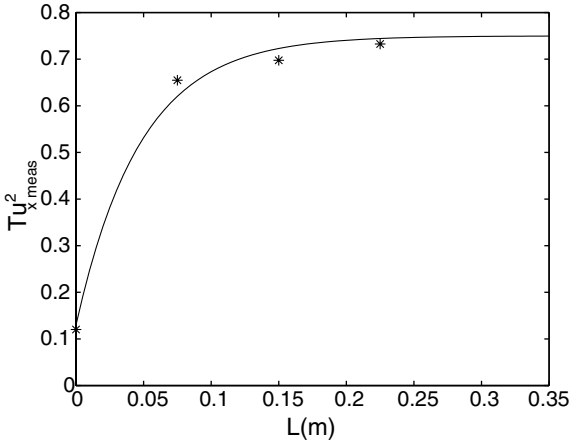

Fig. 5. Turbulence intensity as a function of the length of the porous medium: experimental results (stars) and nonlinear fit (continuous line).

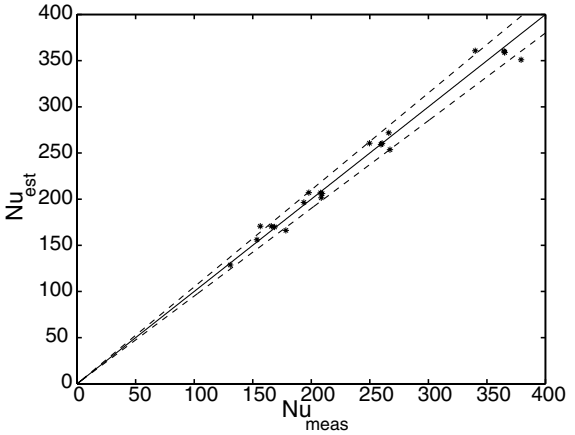

Fig. 6. Nusselt number estimated by the model as a function of the measured Nusselt number.

Results obtained from expression (6) (Nu_{est}) and from experiments (Nu_{meas}) are plotted in Fig. 6. The ±5% deviations from the bisector are also plotted, with dashed lines. Good agreement is obtained showing that the correlation between heat transfer and velocity/turbulence is relevant.

4. Validation of two-dimensional flow

In order to assess the ability of the model to describe airflow through porous media, we then considered a two-dimensional geometry.

4.1. Experimental setup and results

The geometry considered is shown in Fig. 2 except that two baffles covered with half spheres were added (see Fig. 7). The flow path looks like an S-shape. The heating spheres used to estimate the heat transfer coefficient are mainly located near the inlet, on the diagonal and near the outlet. They are numbered from 1 to 9.

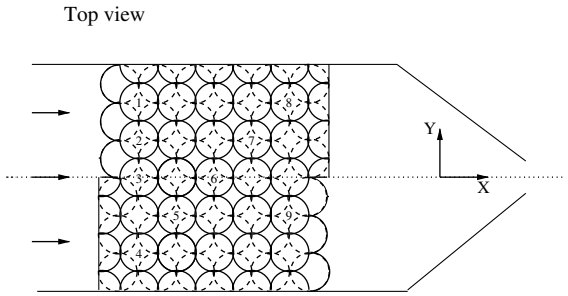

Fig. 7. Flow path with two baffles.

4.2. Simulations

Results are shown in Fig. 8. The pressure drop between the inlet and the outlet was adjusted so as to obtain the correct measured superficial velocity

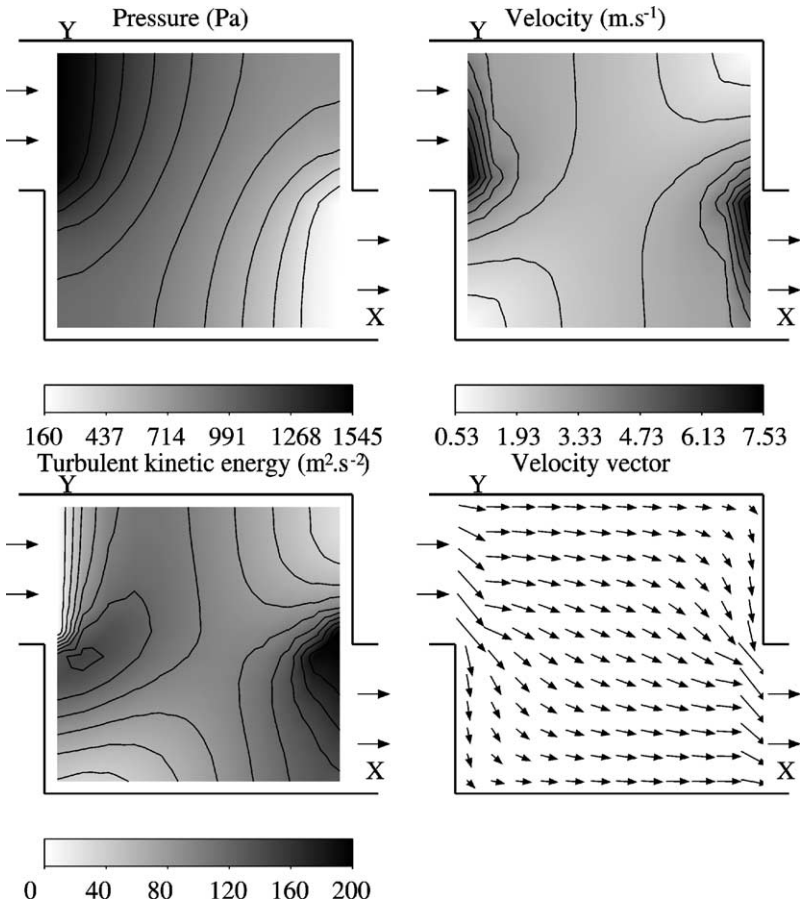

Fig. 8. Pressure, turbulence intensity, superficial velocity magnitude field and vectors in the baffle (continuous lines correspond to isovalue contours).

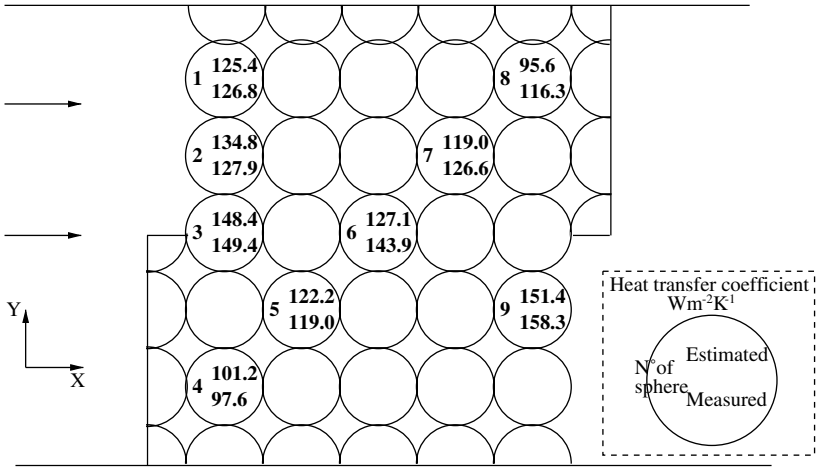

Fig. 9. Heat transfer coefficient measured and estimated by the model.

$v = 2.3\ \mathrm{m\,s^{-1}}$. The pressure field obviously shows a decrease between the inlet and the outlet. As macroscopic inertial terms are neglected, the velocity field is symmetrical. The baffle is responsible for an overspeed of airflow in both the inlet and outlet areas. Turbulence was very low at the inlet as quiet ambient air was introduced into the porous medium. However, turbulent kinetic energy was generated as the flow passes through the porous medium, reaching high values in the outlet section. The velocity fluctuations were then of the same order as the mean interstitial velocity v/ϕ.

Fig. 9 gives a representation of the porous medium and shows the heat transfer coefficient for each heating sphere h estimated from the model (Eq. (15)) (upper value) and measured with the stationary method (lower value). The measured value of h is higher near the outlet (sphere 9) than near the inlet (sphere 2), in agreement with the model, which takes turbulence generation and transport of into account. The difference in this particular case is due only to turbulence as the velocity remains the same between the inlet and the outlet. In addition, both the model and the experiment show that $h(\text{sphere } 3) > h(\text{sphere } 2)$. The increase of h results from a higher velocity value at the edge of the inlet section (sphere 3) than in the middle of the inlet (sphere 2). As far as the diagonal is concerned, $h(\text{sphere } 6) > h(\text{spheres } 5/7) > h(\text{spheres } 4/8)$. Here again, the velocity field (see Fig. 8) gives the explanation: along the diagonal, the velocity reaches its maximum in the middle of the square and decreases towards the corners. Differences between the measurements and the model occur on the diagonal, however, as $h_{\text{measured}}(\text{sphere } 8) > h_{\text{measured}}(\text{spheres } 4)$ and $h_{\text{measured}}(\text{sphere } 7) > h_{\text{measured}} \times (\text{spheres } 5)$, whereas these trends are reversed for the model. The differences probably result from the fact that the model ignores the inertial terms in the momentum equations (see Eq. (2)). Nevertheless, the average relative variation defined as $1/9 \sum_1^9 \frac{|h_{\text{measured}} - h_{\text{estimated}}|}{h_{\text{measured}}}$ is only 5.6%, and predictions from the model can thus be considered as reliable.

5. Conclusion

This article proposes a semi-empirical model to predict the flow field in a porous medium. Calculation of the pressure and velocity fields is based on the Darcy–Forchheimer equation. The turbulent kinetic energy is obtained from a transport equation involving specific source and sink terms for the porous medium. The model has four coefficients, which were identified through wind tunnel experiments using stacked spheres as a porous medium for a one-directional flow.

Heat transfer between the spheres and the air is described by a correlation that links the local Nusselt number to the modified Reynolds number and to turbulence intensity. The three parameters of this thermal model were then identified from the experimental data. The main interest of this model is that it links the heat transfer coefficient to local turbulence. The approach can thus be used for two- or three-dimensional flows.

The model was tested using the identified parameters for two-dimensional flow configuration. Most characteristics of the measured heat transfer coefficients were reproduced and estimated with a relative accuracy of the order of 6%.

References

[1] G. Alvarez, G. Thrystram, Design of a new strategy for the control of the refrigeration process: fruit and vegetables conditioned in a pallet, Food Control 6 (6) (1995) 345–347.

[2] K. Beurkema, S. Bruin, Heat and mass transfer during cooling and storage of agricultural products, Chem. Eng. Sci. 37 (2) (1982) 291–298.
[3] M. Talbot, C. Oliver, J. Gaffney, Pressure and velocity distribution for air flow through fruits packed in shipping containers using porous media analysis, ASAE (1991) 406–417.
[4] V. Morgan, The overall convection heat transfer from smooth circular cylinders, Adv. Heat Transfer 11 (1975) 199–225.
[5] E. Comings, J. Clapp, J. Taylor, Air turbulence and transfer process, Ind. Eng. Chem. 40 (6) (1948) 1076–1082.
[6] J. Lazis, Influence de l'incidence et de la turbulence de l'écoulement amont sur le transfert de chaleur d'un faisceau de tubes à ailettes hélicoïdales, Thèse, Université de Poitiers, 1986.
[7] K. Stephan, D. Traub, Einfluß von Rohrreihenzahl und Anströmturbulenz auf die Wärmeleistung von quer angeströmten Rohrbündeln, Wärme Stoffübertrag. 21 (1987) 103–113.
[8] G. Alvarez, D. Flick, Analysis of heterogeneous cooling of agricultural products inside bins. Part I: aerodynamic study, J. Food Eng. 39 (1999) 227–237.
[9] S. Green, Modelling turbulent air flow in a stand of widely-spaced trees, Phoenics J. 5 (3) (1992) 294–312.
[10] B. Antohe, J. Lage, A general two-equation macroscopic turbulence model for incompressible flow in porous media, Int. J. Heat Mass Transfer 40 (13) (1997) 3013–3024.
[11] N. Nakayama, F. Kuwahara, A macroscopic turbulence model for flow in a porous medium, J. Fluids Eng. 121 (1999) 427–433.
[12] S. Ergun, Fluid flow through packed columns, Chem. Eng. Prog. 48 (2) (1952) 89–94.
[13] H. Kaviany, in: W.M. Rohsenow, J.P. Harnett, Y.I. Cho (Eds.), Heat Transfer in Porous Media in Handbook of Heat Transfer, third ed., McGraw-Hill Handbooks, New York, 1998.
[14] S. Green, Air flow through and above a forest of widely spaced trees, Ph.D. Thesis, University of Edinburgh, 1990.
[15] J.D. Wilson, A second-order closure model for flow through vegetation, Bondary Layer Meteorol. 42 (1988) 371–393.
[16] E. Dyban, E. Epick, L. Kozlava, Combined influence of turbulence intensity and longitudinal scale and air flow acceleration on heat transfer of circular cylinders, in: Fifth Conference of Japanese Society of Mechanical Engineering, 1974, pp. 310–314.
[17] E. Dyban, E. Epick, E. Ya, Some heat transfer features in the air flows of intensified turbulence, in: Proceedings of the 4th Heat Transfer Conference, F.C 5.7, part 2, 1970.
[18] A. Kondjoyan, G. Alvarez, Etude bibliographique sur les coefficients de transferts de chaleur et de matire convectifs entre l'air et un ensemble de produits. du cylindre ou la sphre isols un ensemble de deux quatre de ces objets, Entropie 19 (1995) 1–11.
[19] S. Patankar, Numerical Heat Transfers and Fluid Flow, McGraw-Hill, Hemisphere, Washington DC, 1980.
[20] J. Arce, V. Sweat, Survey of published heat transfer coefficients encountered in food refrigeration process, Trans. ASRHAE 86 (2) (1980) 235–260.
[21] W. Nakayama, H.S.H. Kuwahara, Heat transfer from a tube bank to air/water mist flow, Int. J. Heat Mass Transfer 31 (2) (1988) 449–460.
[22] G. Alvarez, D. Flick, Analysis of heterogeneous cooling of agricultural products inside bins. Part II: thermal study, J. Food Eng. 39 (1999) 239–245.